Journal of Organometallic Chemistry 693 (2008) 2748–2754

Contents lists available at ScienceDirect

Journal of Organometallic Chemistry

journal homepage: www.elsevier.com/locate/jorganchem

N-versus *O*-silylation in *cis*-[(^{t}BuHN)O=P(μ-N^{t}Bu)$_2$P=O(NH^{t}Bu)] and [Me$_2$Si(μ-N^{t}Bu)$_2$P=O(NHPh)]. Solid-state structures of their silylation products, of co-crystalline *cis*-[(^{t}BuHN)O=P(μ-N^{t}Bu)$_2$P=O(NH^{t}Bu)], and of {[Me$_2$Si(μ-N^{t}Bu)$_2$P=O(N(SiMe$_3$)Ph)]VCl$_3$}

Dana C. Haagenson [a], Graham R. Lief [a], Lothar Stahl [a,*], Richard J. Staples [b]

[a] Department of Chemistry, University of North Dakota, Grand Forks, ND 58202-9024, United States
[b] Department of Chemistry and Chemical Biology, Harvard University, Cambridge, MA 09208, United States

ARTICLE INFO

Article history:
Received 15 April 2008
Received in revised form 14 May 2008
Accepted 15 May 2008
Available online 24 May 2008

Keywords:
Diazadiphosphetidines
Diazasilaphosphetidines
O-Silylation
N-Silylation
N,N,N-Phosphoramidates
Vanadium(III)

ABSTRACT

The solid-state structure of *cis*-[(^{t}BuHN)O=P(μ-N^{t}Bu)$_2$P=O(NH^{t}Bu)] (**A**), isolated as a 2-phenyl-2-propanol/2-phenyl-2-propanehydroperoxide co-crystal (**1**), is reported. Treatment of pure **A** with two equivalents of *n*-butyllithium, followed by addition of Me$_3$SiCl, afforded the bis-*O,O′*-silylated *cis*-[(Me$_3$SiO)^{t}BuN=P(μ-N^{t}Bu)$_2$P=N^{t}Bu(OSiMe$_3$)] (**2**), whose solid-state structure was determined. When the cyclic *N,N,N*-phosphoramidate [Me$_2$Si(μ-N^{t}Bu)$_2$P=O(NHPh)] (**B**) was subjected to the same treatment as **A**, however, the *N*-silylated [Me$_2$Si(μ-N^{t}Bu)$_2$P=O(N(SiMe$_3$)Ph)] (**3**), was obtained. Its solid-state structure was determined. The reaction of **3** with VCl$_3$(THF)$_3$ did not produce the intended *N,O*-chelated V(II) complex, but furnished instead the adduct {[Me$_2$Si(μ-N^{t}Bu)$_2$P=O(N(SiMe$_3$)Ph)] VCl$_3$(THF)}, in which **3** binds the trigonal-bipyramidally coordinated vanadium center through its oxygen atom only.

1. Introduction

The trimethylsilyl moiety (–SiMe$_3$) is used extensively to protect protic hydrogens, like N–H and O–H, and to control the stereochemistry in multistep organic syntheses [1–3]. Inorganic and organometallic chemists employ this group both, as a ligand in its own right [4] and as a mild and clean transfer reagent for ligands, because it reacts with certain element chlorides under the elimination of volatile chlorotrimethylsilane [5]. In this latter role the trimethylsilyl group has also proven invaluable for the synthesis of inorganic polymers, such as in the generation of polyphosphazenes from trimethylsilyl-substituted amino-, and iminophosphines [6–10].

Ambidentate ligands, like the bis(*tert*-butylamino)-substituted phosphorus–nitrogen heterocycle **A** [11,12] and the mono(anilino)-substituted phosphorus–silicon–nitrogen heterocycle **B** [13], can coordinate metals in a number of ways. These phosphorus(V) compounds, which may also be considered bis- and mono-(*N,N,N*-phosphoramidates), respectively, can be introduced into their complexes in either their neutral or their anionic forms. Both approaches, however, suffer from disadvantages. Reactions of the neutral phosphoramidates are restricted to metal source materials with reactive metal–halide or metal–alkyl bonds, such as TiCl$_4$ and AlMe$_3$, respectively [14,15]. In their anionic forms, both **A** and **B** are often strongly reducing, leading to a significant amount of metal reduction, rather than metathesis reactions. Besides, the anions are incompatible with some protic solvents.

To introduce **A** and **B** as ligands into transition-metal complexes we sought more soluble and milder starting materials of these compounds. We therefore set out to synthesize the mono- and bis-trimethylsilyl-substituted derivatives of **B** and **A**, respectively. Our investigations showed that while the dianion of **A** is silylated at oxygen, the mono-anion of the close structural analog **B** is silylated at nitrogen. Although these dissimilar outcomes, especially the *N*-silylation over the *O*-silylation, may seem surprising in light of silicon's oxophilicity, they can be rationalized in terms of the overall reaction thermodynamics.

2. Results

The bis(*tert*-butylamino)cyclodiphosph(III)azane *cis*-[(^{t}BuHN)P-(μ-N^{t}Bu)$_2$P(NH^{t}Bu)] (**C**) may be oxidized with oxygen (from organic peroxides), sulfur, and selenium to furnish the homologous phosphorus(V) compounds *cis*-[(^{t}BuHN)E=P(μ-N^{t}Bu)$_2$P=E(NH^{t}Bu)] (E = O, S, Se), respectively [15–19]. Notably, tellurium yields only

* Corresponding author. Fax: +1 701 7772331.
E-mail address: lstahl@chem.und.edu (L. Stahl).

0022-328X/$ - see front matter © 2008 Elsevier B.V. All rights reserved.
doi:10.1016/j.jorganchem.2008.05.023

the mono-oxidation product, namely *cis*-[(^{t}BuHN)Te=P(μ-N^{t}Bu)$_2$-P(NH^{t}Bu)] [20]. The solid-state structures of the disulfide, the diselenide and the monotelluride had been reported, but that of the dioxide was previously unknown.

We discovered that while pure *cis*-[(^{t}BuHN)O=P(μ-N^{t}Bu)$_2$P=O(NH^{t}Bu)] precipitated in microcrystalline form only, co-crystals of this dioxide with the oxidant cumene hydroperoxide and the by-product cumyl alcohol were suitable for single-crystal X-ray analysis. The crystal and refinement data of **1**, as obtained from this study, are listed in Table 1, while Table 2 contains selected bond parameters.

Shown in Fig. 1 is the asymmetric unit of **1**, which consists of one molecule of the cyclodiphosph(V)azane, and one molecule each of the hydroperoxide and alcohol co-crystallants. Co-crystals are common in chemistry, the most widespread examples being solvates and inclusion compounds [21]. Cases such as **1**, however, where the unit cell contains, with the exception of **C**, all reactants and products of a reaction are rare. The Bu^{t}N(H) groups are *endo–endo* configured, namely, both amino-hydrogen atoms are located above the heterocyclic ring. This arrangement is in contrast to the structures of the homologous heavier dichalcogenides, which display *endo–exo* conformations—most likely due to the larger sizes of sulfur and selenium.

The P_2N_2 ring of the bis(*N,N,N*)-phosphoramidate is almost planar, both NPN wedges enclosing a dihedral angle of merely 2.09(9)°. The phosphorus–nitrogen bonds of the four-membered ring have normal lengths, being 1.678(2) Å long on average, while the exocyclic P–N bonds are shorter at 1.622(2) Å, as is typically the case for these molecules [19,22]. The phosphorus–oxygen double bonds (1.467(2) Å) fall into the expected range and so do the remaining bond parameters.

Cumene hydroperoxide, a common oxidizer and an intermediate in the synthesis of phenol and acetone from cumene, is a liquid at room temperature. To our knowledge the crystal structure of cumene hydroperoxide has not been reported; we are also unaware of any X-ray structurally studied co-crystals containing this molecule. The crystal structure of **1**, thus, provides the first opportunity to inspect the bond parameters of this peroxide in the solid state.

Unfortunately, the most interesting part of this molecule, namely the hydroperoxy moiety, O–O–H, is disordered with two conformations, of which only the predominant one is shown in Fig. 1. The carbon–carbon bonds have normal lengths, as does the peroxide bond, which, at 1.460(12) Å, is equidistant with that in H_2O_2, 1.458(4) Å [23].

Table 2
Selected bond lengths (Å) and angles (°) for **1** and **2**

	1	2
P–N(term) avg.	1.622(2)	1.520(2)
P–N(μ) avg.	1.678(2)	1.696(2)
P–O, avg.	1.467(2)	1.592(2)
Si–O, avg.		1.670(2)
Si–C, avg.		1.849(4)
C(23)–O(3)	1.485(4)	
C(32)–O(4)	1.317(12)	
O(4)–O(5)	1.460(12)	
N(μ)–P–N(μ) avg.	84.14(11)	83.86(11)
N(μ)–P–N(term) avg.	111.12(11)	125.74(14)
N(μ)–P–O, avg.	118.46(11)	105.92(11)
P–N(μ)–P, avg.	95.84(11)	95.23(11)
N(term)–P–O, avg.	111.05(11)	106.65(13)
P–O–Si, avg.		134.02(14)
P–N(term)–C, avg.	130.15(19)	137.4(2)

Like cumene hydroperoxide, cumyl alcohol (2-phenyl-2-propanol) has never been subjected to a single-crystal X-ray analysis, although the structure of a dimolybdenum hexaalkoxide complex of this alcohol has been reported [24]. The alcohol was structurally characterized as a co-crystallant in a tin–alkoxide cluster, but the disorder in the nonaromatic portion of the molecule was so severe that the OH and CH_3 groups were indistinguishable [25]. In **1** the alcohol is ordered, and this allowed us to obtain precise bond lengths and angles of this molecule, some of which are listed in Table 2. The aliphatic and aromatic carbon–carbon framework shows no unusual features, and neither does the carbon–oxygen bond, with its typical length of 1.485(4) Å. The cumene hydroperoxide is hydrogen-bonded to one of the phosphoryl oxygen atoms via a strong hydrogen bond (2.614(7) Å), while a weaker, and hence longer, hydrogen bond (2.901(3) Å) connects the alcohol with the second phosphoryl moiety [26] (Scheme 1).

Co-crystalline **1** can be freed of both, cumene hydroperoxide and cumyl alcohol, by washing with hexanes to yield analytically pure **A**. Treatment of **A** with two equivalents of *n*-butyllithium, followed by addition of two equivalents of chlorotrimethylsilane, Scheme 2, afforded disilylated **2** in good yields. Norman and coworkers had previously reported that the dilithiations and subsequent silyl-, germyl-, and stannylations of *trans*-[C_6H_5NHPS-(μ-N^{t}Bu)$_2$PS(NHC$_6$H$_5$)] produced the *N,N′*-disubstituted products [27]. Although the NMR data of **2** supported a symmetrical product, we were unable to discern from these spectra alone whether

Table 1
Crystal, data collection, and refinement data for **1**–**4**

	1	2	3	4
Molecular formula	$C_{34}H_{62}N_4O_5P_2$	$C_{22}H_{54}N_4O_2P_2Si_2$	$C_{19}H_{38}N_3OPSi_2$	$C_{23}H_{46}Cl_3N_3O_2PSi_2V$
Formula weight	668.82	524.81	411.67	641.07
Space group	*Pbca* (no. 61)	*C*2/*c* (no. 15)	*P*2$_1$/*c* (no. 14)	*P*2$_1$/*n* (no. 14)
T (K)	213	213	213	213
a (Å)	15.6840(17)	10.0283(13)	9.6531(9)	9.8603(12)
b (Å)	21.9943(12)	16.9911(13)	12.1954(11)	19.273(3)
c (Å)	22.7020(12)	19.7028(18)	20.7594(19)	17.341(2)
β (°)		103.270(3)	98.584(2)	90.198(3)
V (Å^3)	7831.3(7)	3267.6(6)	2416.5(2)	3295.4(7)
Z	8	4	4	4
λ (Å)	0.71073	0.71073	0.71073	0.71073
ρ_{calc} (g cm^{-3})	1.135	1.067	1.132	1.292
μ (mm^{-1})	0.152	0.229	0.226	0.690
Reflections collected	47 040	9680	14 778	21 887
Independent reflections (R_{int})	8547 (0.0553)	3398 (0.0399)	5145 (0.0220)	7989 (0.0911)
Parameters	420	145	235	317
$R(F)$[a] [$I > 2\sigma(I)$]	0.0637	0.0666	0.0432	0.0826
$wR_2(F^2)$[b] [all data]	0.1862	0.1802	0.1347	0.2210

[a] $R = \sum|F_o - F_c|/\sum|F_o|$.
[b] $R_w = \{[\sum w(F_o^2 - F_c)^2/[\sum w(F_o^2)^2]\}^{1/2}$; $w = 1/[\sigma^2(F_o)^2 + (xP)^2 + yP]$ where $P = (F_o^2 + 2F_c^2)/3$.

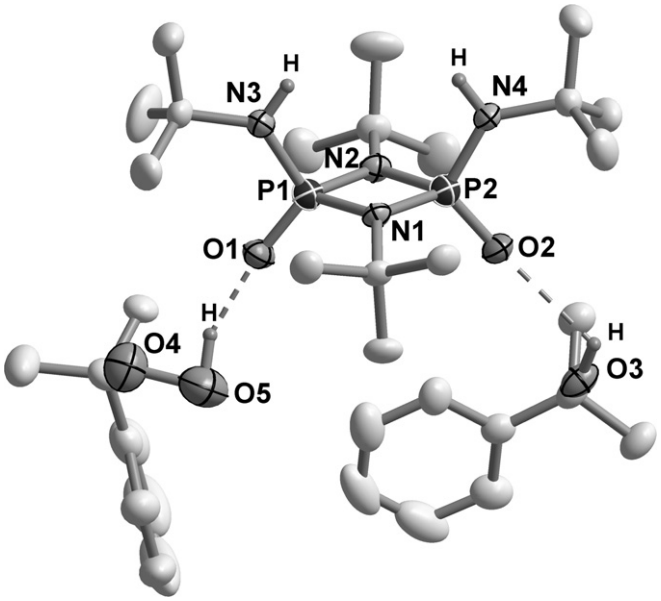

Fig. 1. Asymmetric unit and partial labeling scheme of **1**. The thermal ellipsoids are drawn at the 35% probability level. With the exception of the amino- and hydroxyl hydrogens, all hydrogen atoms have been omitted to improve clarity. Hydrogen bonds are indicated by dashed lines.

the trimethylsilyl groups were attached to the oxygen or the nitrogen atoms. We therefore conducted an X-ray analysis on single crystals of **2**, the results of which are shown in Fig. 2. The crystal and data collection parameters obtained from this study are listed in Table 1, while Table 2 contains selected bond parameters.

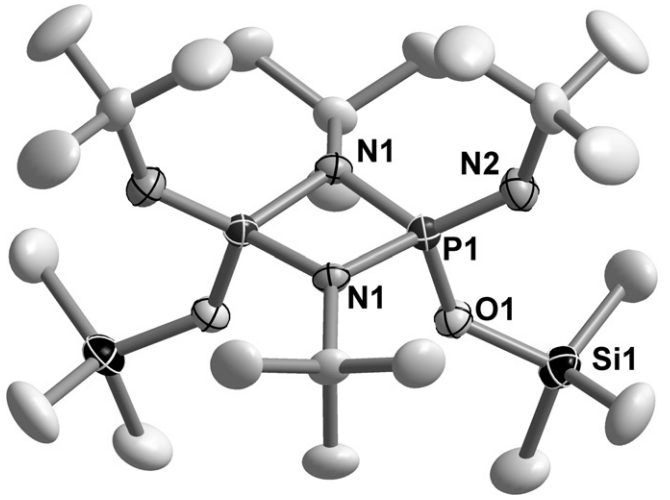

Fig. 2. Solid-state structure and partial labeling scheme of **2**. Thermal ellipsoids are drawn at the 50% probability level, and the hydrogen atoms have been omitted for improved clarity.

As Fig. 2 shows, and in notable contrast to the results obtained by Norman et al., the product obtained from this reaction is the *O*,*O*′-disilylated isomer. The molecules are located on the twofold rotation axes of the space group *C*2/*c* and are, thus, rigorously C_2 symmetric. This bis(*N*,*N*,*N*-phosphoramidate) consists of an inorganic O(N═P(μ-N)$_2$P═N)O core that is studded with four *tert*-butyl groups and two trimethylsilyl groups. The substantial steric repulsions of these bulky attachments dictate their relative conformations. Thus, the *tert*-butyl substituents of the imino-nitrogen atoms (N2) have *endo*-conformations, whereas the trimethylsilyl

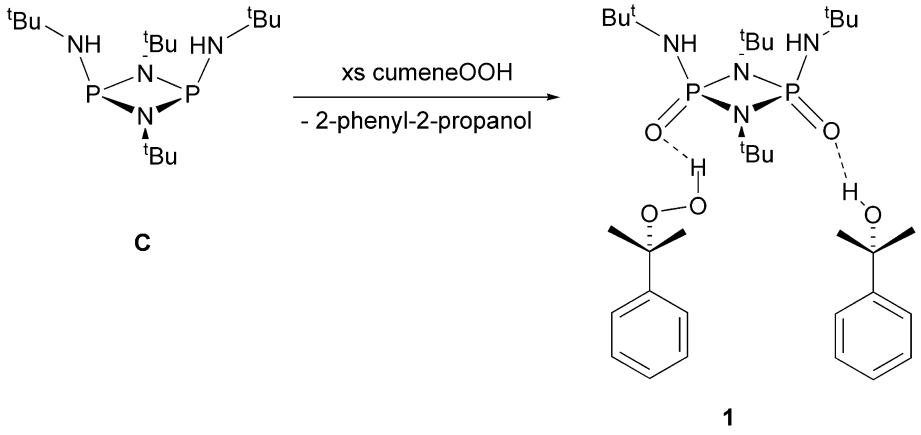

Scheme 1.

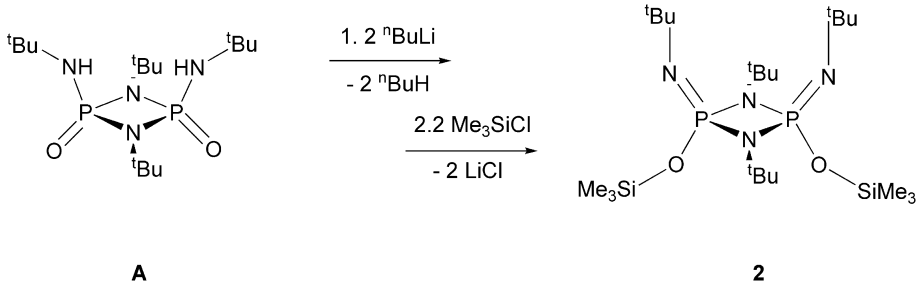

Scheme 2.

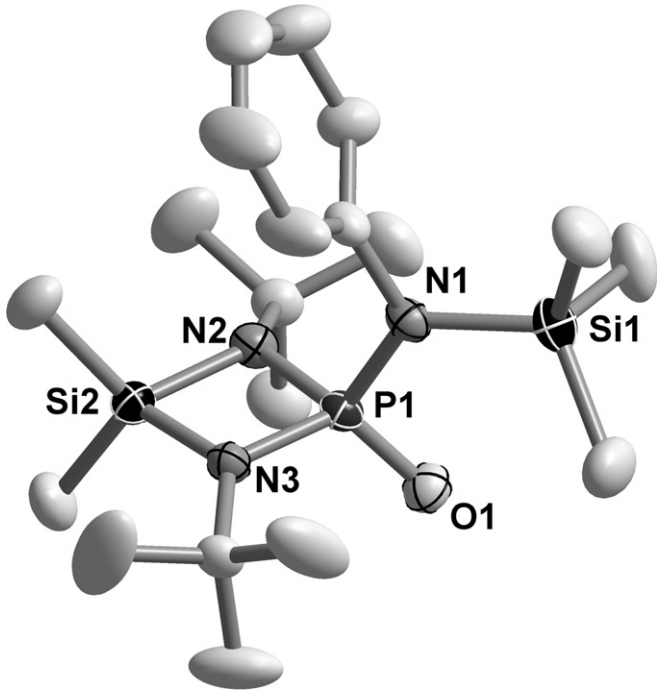

Fig. 3. Thermal-ellipsoid (50% probability) plot and partial labeling scheme of **3**. Hydrogen atoms have been omitted to improve clarity.

Table 3
Selected bond lengths (Å) and angles (°) for **3** and **4**

	3	4
P–N(term)	1.6706(15)	1.664(6)
P–N(μ) avg.	1.6700(15)	1.648(5)
Si–N(μ) avg.	1.7432(16)	1.750(5)
Si–N(term)	1.7708(17)	1.774(5)
P–O	1.4753(14)	1.496(4)
V–Cl, avg.		2.2419(18)
V–O(P=O)		1.990(4)
V–O(THF)		2.145(4)
N(term)–P–N(μ) avg.	110.75(8)	113.2(3)
N(term)–P–O	107.57(8)	104.0(2)
N(μ)–P–O	119.40(8)	118.9(2)
N–Si–N	83.30(7)	82.5(2)
Si–N(term)–P	122.60(9)	126.8(3)
O(1)–V(1)–O(2)		175.73(17)
Cl(1)–V(1)–Cl(2)		124.09(8)
Cl(2)–V(1)–Cl(3)		118.08(8)
Cl(1)–V(1)–Cl(3)		116.31(8)
O(1)–V(1)–Cl, avg.		94.13(13)
O(2)–V(1)–Cl, avg.		85.96(13)

groups, with their longer N–Si bonds, are disposed in an exo fashion. Due to the intramolecular repulsion of their *tert*-butyl substituents, the separation of the exocyclic nitrogen atoms (5.099 Å) is much larger than that of the oxygen atoms (3.317 Å). The silylations have converted the P–O double bonds to single bonds, while P1 and N1 are now connected by a double bond. These changes are reflected in phosphorus–nitrogen bonds that have shortened from 1.622(2) Å in **1** to 1.520(2) Å in **2**. Analogously, the P–O bonds have lengthened from 1.467(2) to 1.592(2) Å, while the newly-formed Si–O bonds are 1.670(2) Å long—a typical bond length for silicon–oxygen single bonds.

The metric parameters of the heterocycle changed but little during the chemical transformation from **1** to **2**. Thus, the P–N bonds are only slightly longer in **2** (1.696(2) vs. 1.678(2) Å in **1**), while all the endocyclic angles of this ring remained virtually unchanged.

We then carried the silylation reaction sequence out on **B**, a mono-*N*,*N*,*N* phosphoramidate in which the exocyclic nitrogen atom bears a phenyl, rather than a *tert*-butyl, substituent. The NMR spectral analysis revealed that here, too, only one product (**3**) had formed, but the spectra were again inconclusive regarding the position of the trimethylsilyl group. A single-crystal X-ray study showed (Fig. 3) that in this reaction the *N*-silylated phosphoramidate, **3**, had been produced. Its crystal and refinement data are listed in Table 1, while Table 3 contains selected bond parameters (Scheme 3).

To test the utility of these silylated phosphoramidates as ligand transfer reagents, we treated a toluene solution of $VCl_3(THF)_3$ with **3**, as shown in Scheme 4. Despite extended reaction times (12 h, 50 °C), however, we were unable to observe any signs of chlorotrimethylsilane elimination. Instead, we isolated the vanadium complex **4**, as an adduct of **3** with VCl_3(THF).

Fig. 4 shows the solid-state structure of **4**, while selected crystal- and refinement data, and bond parameters are listed in Tables 1and 3, respectively. The vanadium(III) complex has a trigonal-bipyramidal coordination geometry, with the chloride ligands occupying the equatorial plane, while the two-oxygen donor ligands (**3** and THF) are in the axial positions. The vanadium–chloride bonds are, on average, 2.2419(18) Å long, a value that agrees well with the lengths of such bonds in similar complexes [28]. The bond angles are close to those expected for trigonal-bipyramidal geometry, with an almost linear O–V–O arrangement of 175.73(17)° and Cl–V–Cl angles that range from 116.31(8)° to 124.09(8)°. The V–O bonds are decidedly different in length, the donor bond with the sp^2-hybridized oxygen atom (O1) being substantially shorter (1.990(4) Å) than that with the THF ligand, which is rather long at 2.145(4) Å. Steric factors appear to control the conformations of both *O*-donor ligands with respect to the VCl_3 moi-

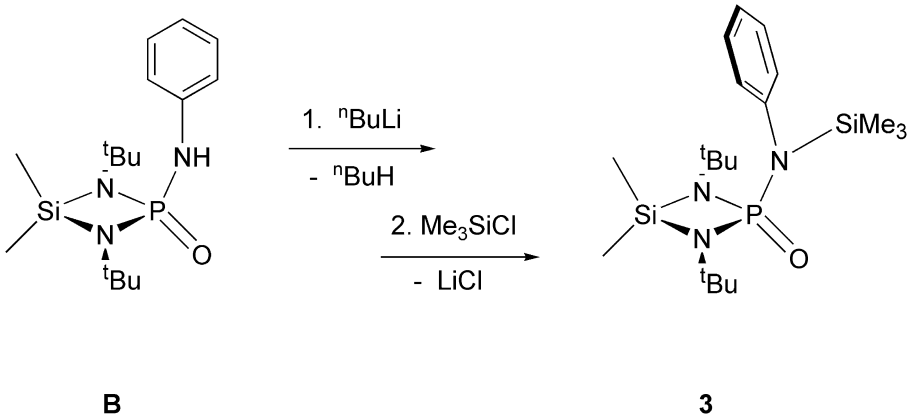

B **3**

Scheme 3.

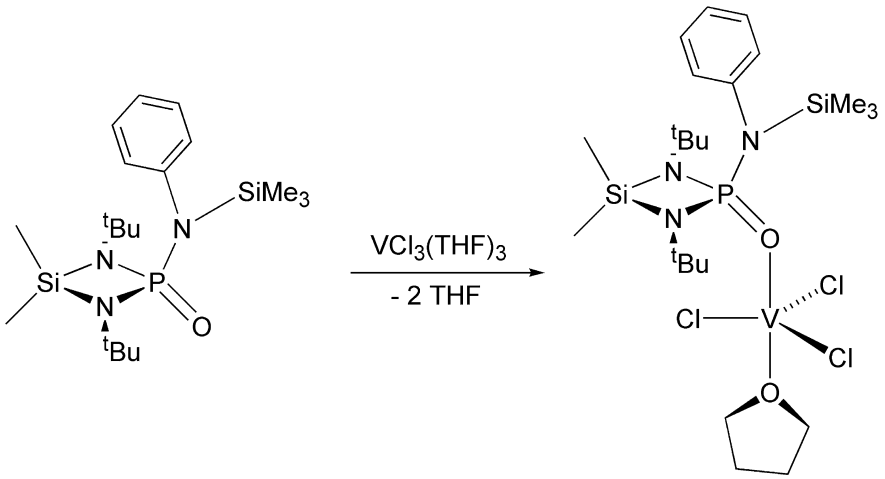

3 4

Scheme 4.

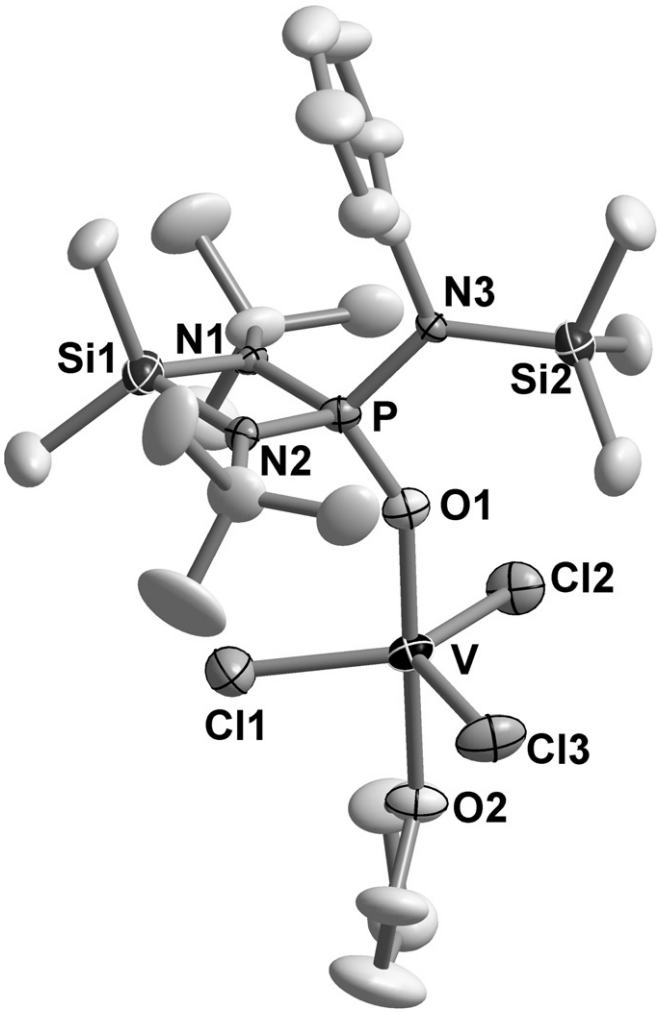

Fig. 4. Thermal ellipsoid plot and partial labeling scheme of **4**. The thermal ellipsoids are drawn at the 50% probability level and all hydrogen atoms have been omitted for clarity.

ety. For example, ligand **3** is disposed in such a manner that its sterically least-demanding feature, namely the four-membered ring, straddles one of the V–Cl bonds. The bulkiest substituents of the ligand, the *tert*-butyl groups, in turn, dip between the chloride ligands, while the THF ligand bisects two of the Cl–V–Cl angles.

Although the attempted *N*,*O* ligation of vanadium by **3** failed under the conditions employed by us, the structure of **4** is nonetheless interesting because it presumably represents an intermediate in the reaction coordinate to the targeted product. More forcing conditions are likely necessary to effect the desired chlorotrimethylsilane elimination and the ligation of the vanadium ion by **3** in a bidentate-chelating manner.

3. Discussion

Because of their ambidenticity phosphoramidates may be silylated at either nitrogen or oxygen, and examples of both isomers have been reported in the literature [29,30]. The silylations of the phosphoramidates **A** and **B** with Me_3SiCl yielded the bis-*O*-silylated product (**2**) in the former and the mono-*N*-silylated product (**3**) in the latter. While the dissimilar outcomes of these reactions might be rationalized in terms of kinetic versus thermodynamic control, both, the *O*,*O*′-disilyl derivative, **2**, and the *N*-silyl derivative, **3**, are thermodynamic products.

Silicon has an exceptionally high affinity for oxygen, the silicon–oxygen single bond (445 kJ mol^{-1}) being among the strongest single bonds known; it is ca. 90 kJ mol^{-1} stronger than the analogous silicon–nitrogen bond [30]. This substantial energy difference dictates that in ambidentate molecules having both –OH and –NH groups, silylation usually occurs at oxygen, as long as steric and kinetic effects are negligible. We hasten to point out, however, that silylations are considerably more complex than suggested here, as numerous experimental and computational studies have shown [31–35] (Chart 1).

In phosphoramidates, by contrast, where silylation may also occur at either nitrogen or oxygen, the overall thermodynamics are quite different. Because the conversion of the phosphoryl bond (620 kJ mol^{-1}) to a phosphorus–oxygen single bond (368 kJ mol^{-1}) exacts a significant thermodynamic penalty, phosphoramidates are usually silylated at nitrogen. The bond-enthalpy changes accompanying phosphoramidate metallations with element trihalides were studied in detail by Glidewell and Duncan [36,37]. Because compounds **2** and **3** are thermodynamic products they are amenable to the same bond-enthalpy estimates used by these researchers, whose estimated bond enthalpies we adopt here. In Chart 2 we contrast the two conceivable structural isomers for silylated phos-

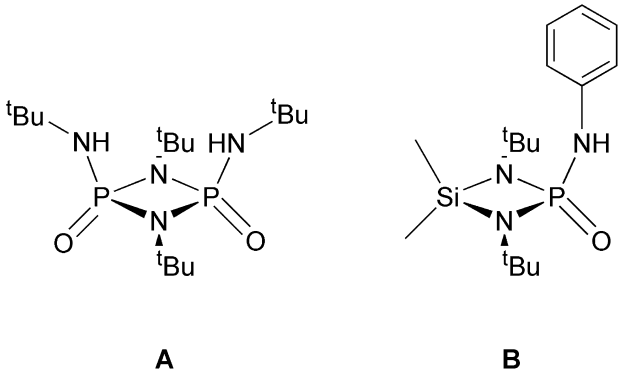

Chart 1.

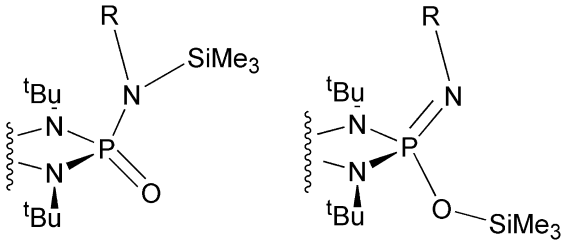

Chart 2.

Table 4
Relevant bond enthalpies for **2** and **3**, as obtained from Ref. [15]

2	kJ mol^{-1}	**3**	kJ mol^{-1}
Si–N	335	Si–O	445
P–N	347	P=N	459
P=O	620	P–O	368
Σ	1302	Σ	1272

phoramidates, while we list the relevant estimated bond enthalpies and their sums for each isomer in Table 4.

Discounting steric factors, and focusing strictly on bond enthalpies, *N*-silylation is favored over *O*-silylation by approximately 30 kJ mol^{-1} per P=O(N) moiety. This thermodynamic estimate is supported by synthetic studies where *N*-silylated products predominate [36]. If the nitrogen atom bears any steric bulk at all, however, the energy differences between both isomers are substantially smaller. Thus, for example, based on variable-temperature NMR studies, it was estimated that an *N*,*O*,*O*-triphenylphosphoramidate was only 7.1 kJ mol^{-1} more stable than the corresponding *O*-silylated derivative [30]. Because of the low activation energies for 1,3-*N*,*O*-trimethylsilyl migrations such small energy differences between isomeric *N*- and *O*-silylated isomers usually manifest themselves in fluxional molecules [29,30].

Therefore, in contrast to most silylation reactions, phosphoramidates are typically silylated at nitrogen, making the *N*-silylated **3** the "conventional" product, while the *O*-silylated **2** is the "unconventional" product. The absence of any fluxionality in the bis (*O*-silylated) **2** further confirms that it must be substantially more stable than the alternative bis(*N*,*N*′-silylated) isomer. It is easy to see why this might be the case, because a bis(*N*,*N*′-silylated) derivative (Chart 3) would suffer from excessive steric strain due to no less than three repulsive interactions. The existence of isomer **2** is a reminder that non-bonding interactions can play as large, if not a larger, role than covalent bonds, even in the selection of thermodynamic products.

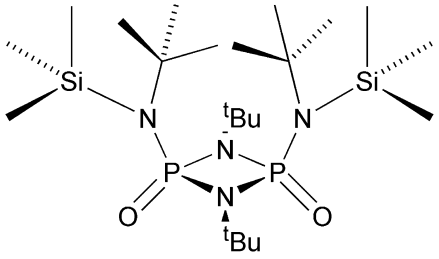

Chart 3.

4. Summary

Contrary to conventional assumptions about the oxophilicity of silicon, phosphoramidates are preferentially silylated at nitrogen, because this structural isomer preserves the strong phosphorus–oxygen double bond of these molecules. If the nitrogen atom of these ambidentate molecules bears significant steric bulk, however, the *O*-silylated isomer may be the thermodynamically more stable product.

Although the trimethylsilyl-derivatized phosphoramidates **2** and **3** proved unsuitable as ligand transfer reagents to transition metal under mild conditions, they may find uses in transformations involving the more reactive metalloid- and nonmetal halides, such as $SiCl_4$ and PCl_3.

5. Experimental

All experiments were performed under an atmosphere of purified nitrogen or argon, using standard Schlenk techniques. Solvents were dried and freed of molecular oxygen by distillation under an atmosphere of nitrogen from sodium or potassium benzophenone ketyl immediately before use. NMR spectra were recorded on a Bruker AVANCE-500 NMR spectrometer. The ^{1}H, ^{13}C, ^{29}Si, and ^{31}P NMR spectra are referenced relative to C_6D_5H (7.15 ppm), C_6D_6 (128.0 ppm), TMS (0.0 ppm) and $P(OEt)_3$ (137.0 ppm), respectively. Melting points were obtained on a Mel-Temp apparatus; they are uncorrected. Elemental analyses were performed by E and R Microanalytical Services, Parsipanny, NJ.

Chlorotrimethylsilane and cumene hydroperoxide were purchased from Petrarch and Aldrich, respectively; they were used as received. The heterocycles [$Me_2Si(\mu$-$N^tBu)_2P$=O(NHPh)] [38] and *cis*-[(^{t}BuHN)O=P(μ-$N^tBu)_2$P=O(NH^tBu)] [15] were synthesized according to published procedures.

6. Syntheses

6.1. *cis*-[(Me_3SiO)^{t}BuN=P(μ-$N^tBu)_2$P=$N^tBu(OSiMe_3)$] (**2**)

A two-necked, 100 mL round-bottomed flask equipped with a dropping funnel, inlet, and stirbar, was charged with **1** (2.46 g, 6.48 mmol). This white solid was suspended in 30 mL of hexanes. Then *n*-butyllithium (1.88 mL, 7.70 mmol) in 5 mL THF was added dropwise, and the resulting yellow solution was heated to reflux for 1 h. The solution was then allowed to cool to room temperature and Me_3SiCl (0.60 mL, 4.7 mmol) in 5 mL of hexanes was added dropwise with vigorous stirring. The resulting milky-white mixture was warmed to 50 °C and kept at that temperature for 16 h. All liquids were removed *in vacuo* and the colorless solid was extracted with 30 mL of hexanes, filtered on a fine frit and concentrated to half its volume. After the clear, colorless solution had been kept in a −21 °C freezer for 2 days, colorless needles (0.891 g) formed. Yield: 72.1%.

M.p.: 122 °C dec. ^{1}H NMR (500.13 MHz, benzene-d_6, 26 °C) δ = 1.49 (s, 18H, N^{t}Bu), 1.46 (s, 18H, N^{t}Bu), 0.36 (s, 18H, SiMe$_3$). ^{13}C{^{1}H} NMR (125.76 MHz, benzene-d_6, 26 °C) δ = 53.6 (s, N^{t}Bu), 51.0 (s, N^{t}Bu), 34.7 (t, J_{PC} = 5.97 Hz, N^{t}Bu), 31.3 (t, J_{PC} = 4.72 Hz, N^{t}Bu), 1.76 (s, SiMe$_3$). ^{31}P{^{1}H} NMR (202.46 MHz, benzene-d_6, 26 °C) δ = −42.15 (s). Anal. Calc. for $C_{22}H_{54}N_4P_2O_2Si_2$: C, 50.35; H, 10.37; N, 10.67. Found: C, 50.02; H, 10.10; N, 10.81%.

6.2. [Me$_2$Si(μ-N^{t}Bu)$_2$P═O{N(SiMe$_3$Ph)}] (**3**)

A sample of [Me$_2$Si(μ-N^{t}Bu)$_2$P═O(NHPh)] (2.24 g, 6.60 mmol), dissolved in 20 mL of toluene, was treated with *n*-butyllithium (4.4 mL, 7.0 mmol, 1.6 M) dropwise at 0 °C. The solution remained clear and colorless while it was refluxed for 1 h. Chlorotrimethylsilane (0.89 mL, 7.0 mmol), dissolved in 5 mL of toluene, was added dropwise to this solution at room temperature. The mixture was refluxed for 16 h, during which time a white precipitate formed. The solution was then filtered through a medium-porosity frit and concentrated to dryness *in vacuo*. The remaining solid was extracted with hexanes, filtered and stored at −21 °C. Several crops of colorless crystals yielded 2.14 g (79.0%) of product.

M.p.: 98–100 °C. ^{1}H NMR (500.13 MHz, benzene-d_6, 26 °C) δ 7.30 (d, 2H, J = 8.0 Hz, *o*-Ph), 7.08 (t, 2H, J = 7.6 Hz, *m*-Ph), 6.98 (td, 1H, J = 7.4 Hz, *p*-Ph), 1.32 (s, 18H, N^{t}Bu), 0.39 (s, 9H, SiMe$_3$), 0.24 (s, 3H, SiMe), −0.52 (s, 3H, SiMe). ^{13}C{^{1}H} NMR (125.76 MHz, benzene-d_6, 26 °C) δ 144.2 (d, J = 2.6 Hz, Ph), 131.0 (d, J = 3.5 Hz, Ph), 128.2 (s, Ph), 125.3 (d, J = 1.4 Hz, Ph), 52.2 (s, *C*Me$_3$), 32.4 (d, J_{PC} = 2.0 Hz, *CMe*$_3$), 4.2 (s, SiMe), 2.9 (s, SiMe$_3$), 0.9 (d, J = 5.5 Hz, SiMe). ^{31}P{H} NMR (202.46 MHz, benzene-d_6, 26 °C) δ 9.7 (s), ^{29}Si NMR (99.4 MHz, benzene-d_6, 26 °C) δ 9.1 (d, J = 7.2 Hz), −2.6 (s). Anal. Calc. for $C_{19}H_{38}N_3OPSi_2$: C, 55.43; H, 9.30; N, 10.21. Found: C, 55.52; H, 9.47; N, 9.97%.

6.3. {[Me$_2$Si(μ-N^{t}Bu)$_2$P═O(N(SiMe$_3$)Ph)]VCl$_3$(THF)} (**4**)

In a 100-mL, three-necked flask, equipped with a dropping funnel, inert gas inlet and magnetic stir bar, 0.380 g (1.02 mmol) of $VCl_3 \cdot (THF)_3$ and 10 mL of toluene were combined to afford a purple suspension. To this mixture was added via dropping funnel a solution of **3** (0.410 g, 0.996 mmol) in 20 mL of toluene. The reaction mixture was heated to 50 °C and kept at that temperature for 15 h, during which time a deep-blue solution formed. The solution was filtered, concentrated *in vacuo* and stored in a freezer for 2 days. An initial crop of purple crystals (unreacted $VCl_3 \cdot (THF)_3$) was discarded. The supernatant yielded a second crop of deep-blue crystals, which was identified as **4**, (0.377 g, 0.588 mmol). Yield: 59.0%. M.p.: 278 °C dec. Anal. Calc. for $C_{23}H_{46}Cl_3N_3PO_2Si_2V$: C, 43.09; H, 7.23; N, 6.55. Found: C, 42.78; H, 7.01; N, 6.77%.

7. X-ray crystallography

7.1. Compounds ***1***, ***2***, ***3***, and ***4***

A sample of **A** was synthesized as previously reported [15]. Single crystals of **1** were obtained when the reaction mixture was concentrated in vacuo and stored at −20 °C for 5 days. Suitable, single crystals were coated with oil, attached to a glass capillary, and centered on the diffractometer in a stream of cold nitrogen. Reflection intensities were collected with a Bruker SMART CCD diffractometer, equipped with an LT-2 low-temperature apparatus, operating at 213 K. Data were measured using ω scans of 0.3° per frame for 30 s until a complete hemisphere had been collected. The first 50 frames were recollected at the end of the data collection to monitor for decay. Cell parameters were retrieved using SMART [39] software and refined with SAINT [40] on all observed reflections. Data were reduced with SAINT, which corrects for Lp and decay. An empirical absorption correction was applied with SADABS [41]. The structures were solved by direct methods with the SHELXS-90 [42] program and refined by full-matrix least squares methods on F^2 with SHELXL-97 [43], incorporated in SHELXTL-PC, Version 5.03 [44].

Appendix A. Supplementary material

CCDC 680343, 680344, 680345, and 680346 contain the supplementary crystallographic data for **1**, **2**, **3**, and **4**. These data can be obtained free of charge from The Cambridge Crystallographic Data Centre via www.ccdc.cam.ac.uk/data_request/cif Supplementary data associated with this article can be found, in the online version, at doi:10.1016/j.jorganchem.2008.05.023.

References

[1] P.G.M. Wuts, T.W. Greene, Protective Groups in Organic Synthesis, 4th ed., Wiley Interscience, New York, NY, 2006.
[2] P.J. Kocienski, Protecting Groups, 3rd ed., Thieme, Stuttgart, 2005.
[3] J.R. Hwu, N. Wang, Chem. Rev. 89 (1989) 1599.
[4] T.D. Tilley, in: S. Patai (Ed.), The Chemistry of Organic Silicon Compounds, vol. 2, Wiley, Chichester, 1989, p. 1415.
[5] M. Yoshifuji, K. Toyota, in: Z. Rappoport, Y. Apeloig (Eds.), The Chemistry of Organic Silicon Compounds, vol. 3, Wiley, New York, 2001, p. 491.
[6] B. Wang, E. Rivard, I. Manners, Inorg. Chem. 41 (2002) 1690.
[7] P. Wisian-Neilson, R.H. Neilson, J. Am. Chem. Soc. 102 (1980) 2848.
[8] R.C. Samuel, R.P. Kashyap, M. Krawiec, W.H. Watson, R.H. Neilson, Inorg. Chem. 41 (2002) 7113.
[9] J.J. Longlet, S.G. Bodige, W.H. Watson, R.H. Neilson, Inorg. Chem. 41 (2002) 6507.
[10] C. Prieto, C.E. Davis, J.T. Shore, R.H. Neilson, Inorg. Chem. 33 (1994) 5151.
[11] R.R. Holmes, J.A. Forstner, Inorg. Chem. 2 (1963) 380.
[12] I. Schranz, L. Stahl, R.J. Staples, Inorg. Chem. 37 (1998) 1493.
[13] O.J. Scherer, M. Püttmann, C. Krüger, H. Wolmershäuser, Chem. Ber. 115 (1982) 2076.
[14] M. Rastätter, P.W. Roesky, D. Gudat, G.B. Gudat, P.C. Junk, Chem. Eur. J. 13 (2007) 7410.
[15] G.R. Lief, C.J. Carrow, L. Stahl, R.J. Staples, Organometallics 20 (2001) 1629.
[16] T.G. Hill, R.C. Haltiwanger, M.L. Thompson, S.A. Katz, A.D. Norman, Inorg. Chem. 33 (1994) 1770.
[17] T. Chivers, M. Krahn, G. Schatte, Inorg. Chem. 41 (2002) 4348.
[18] T. Chivers, M. Krahn, M. Parvez, Chem. Commun. (2000) 463.
[19] G.G. Briand, T. Chivers, M. Krahn, Coord. Chem. Rev. 233–234 (2002) 237.
[20] G.G. Briand, T. Chivers, M. Parvez, G. Schatte, Inorg. Chem. 42 (2003) 525.
[21] J.D. Dunitz, CrystEngComm 5 (2003) 506.
[22] L. Stahl, Coord. Chem. Rev. 210 (1999) 203.
[23] J.-M. Savariault, M.S. Lehmann, J. Am. Chem. Soc. 102 (1980) 1298.
[24] T.M. Gilbert, C.B. Bauer, A.H. Bond, R.D. Rogers, Polyhedron 18 (1999) 1293.
[25] G.D. Smith, P.E. Fanwick, I.P. Rothwell, Acta Crystallogr., Sect. C C51 (1995) 2501.
[26] G.A. Jeffrey, An Introduction to Hydrogen Bonding, Oxford, New York, 1997.
[27] M.D. Noirot, E.G. Bent, A.D. Norman, Phosphorus Sulfur Silicon 62 (1991) 177.
[28] N. Desmangles, S. Gambarotta, C. Bensimon, S. Davis, H. Zabalka, J. Organomet. Chem. 562 (1998) 53;
P. Berno, S. Gambarotta, S. Kotila, G. Erker, Chem. Commun. (1996) 779.
[29] L. Riesel, A. Claussnitzer, C. Ruby, Z. Anorg. Allg. Chem. 433 (1977) 200.
[30] P.K.G. Hodgson, R. Katz, G. Zon, J. Organomet. Chem. 117 (1976) C63.
[31] S. Kliem, U. Klingebiel, S. Schmatz, J. Organomet. Chem. 686 (2003) 16.
[32] S. Kliem, U. Klingebiel, M. Noltemeyer, S. Schmatz, J. Organomet. Chem. 690 (2005) 1100.
[33] F. Diedrich, U. Klingebiel, M. Schäfer, J. Organomet. Chem. 588 (1999) 242.
[34] R. Wolfgramm, T. Müller, U. Klingebiel, Organometallics 17 (1998) 3222.
[35] R. West, M. Ishikawa, S. Murai, J. Am. Chem. Soc. 90 (1968) 727.
[36] I.A. Duncan, C. Glidewell, J. Organomet. Chem. 97 (1975) 51.
[37] C. Glidewell, J. Organomet. Chem. 108 (1976) 335.
[38] D.C. Haagenson, D.F. Moser, L. Stahl, R.J. Staples, Inorg. Chem. (2002) 1245.
[39] SMART V 4.043, Software for the CCD Detector System, Bruker Analytical X-ray Systems, Madison.
[40] SAINT V 4.035, Software for the CCD Detector System, Bruker Analytical X-ray Systems, Madison, WI, 1995.
[41] SADABS program for absorption corrections using the Bruker CCD Detector System. Based on: R. Blessing, Acta Crystallogr., Sect. A 51 (1995) 33.
[42] G.M. Sheldrick, SHELXS-90, Program for the Solution of Crystal Structures, University of Göttingen, Germany, 1990.
[43] G.M. Sheldrick, SHELXL-97, Program for the Solution of Crystal Structures, University of Göttingen, Germany, 1997.
[44] SHELXTL 5.10 (PC-Version), Siemens Analytical X-ray Instruments, Inc., Madison, WI, 1998.